MoS_2 Doping Using Potassium Iodide for Reliable Contacts and Efficient FET Operation

Kuruva Hemanjaneyulu, Jeevesh Kumar, and Mayank Shrivastava, *Senior Member, IEEE*

***Abstract*— In this paper, we have demonstrated few-layer MoS_2 doping using potassium iodide (KI) solution to realize stable/reliable ohmic contacts and achieve efficient electron transport. We have shown that KI doping allows MoS_2 doping with a dopant density up to 1×10^{12} cm^{-2} near source/drain edge. The same has been explained using density-functional-theory (DFT)-based band structure calculations. KI doping of MoS_2 resulted in contact resistance reduction by 3.5× (0.75 kΩ-μm). The proposed technique and improved contacts have also resulted in 2× improvement in ON-state current (500 μA/μm), transconductance and field-effect mobility (70 cm^2/Vs) without compromising with OFF-state behavior, while maintaining ON to OFF ratio well above 10^6. The reproducibility of the transistor characteristics after a longer period (2 months) confirms the stability of proposed doping technique against environmental conditions.**

***Index Terms*— MoS_2 doping, MoS_2 FETs, potassium iodide (KI) treatment, surface charge transfer doping, transition metal dichalcogenide (TMD) doping.**

I. Introduction

IN LESS than a decade, there have been intensive investigations on various 2D materials such as graphene and transition metal dichalcogenides (TMDs), which is attributed to their extremely flat surfaces having ultrathin layered structure and unique electrical as well as optoelectronic properties. Graphene, on the one hand, has shown great potential for terahertz applications due to the highest carrier mobility and very high sheet carrier concentration [1]–[3]; on the other hand, due to its semimetallic nature, has inhibited switching applications requiring very high ON to OFF ratio ($>10^5$). Lack of switching capability of Graphene FET has led to a shift in interest toward TMDs, a class of semiconducting layered materials [4], attributed to its finite bandgap. Among various TMDs, MoS_2 so far has been the most explored material due to its relative abundance, higher carrier mobility, and promising electronic [5] as well as optoelectronic properties [5]. This has made it a good choice for logic as replacement of Si CMOS, flexible electronics [6]–[8], optoelectronics, and gas-sensing [9] applications.

Like any emerging technology, MoS_2 progress also suffers from technological challenges like large area single-crystal growth, oxide growth over atomically smooth TMD surface, stability and sensitivity toward environmental conditions, and ohmic contacts with stable doping. Realizing ohmic contacts with stable doping and least contact resistance is considered to be among the greatest bottlenecks, which directly limits the carrier transport and channel performance [10]. For ohmic contacts with minimum contact resistance, doping under or around source/drain region is the commonly adopted technique. The stability of the introduced charge from doping is also critical for controlling channel conductivity and variability. The conventional method of ion implantation, which is commonly used in Si CMOS, introduces unrecoverable damage to the 2D material surface and its bulk. This makes ion implantation an unsuitable technique for doping 2D materials. For 2D semiconductors, an efficient way to dope is by surface charge transfer [11], which keeps the crystal and the surface properties intact. Surface charge transfer doping technique has been demonstrated recently for MoS_2, while using potassium metal [12], benzyl viologen [13], [14], metal nanoparticles [15], $Cs(CO)_3$ [16], metal ions [17], and gold chloride solution [13], [18]. It should, however, be noted that most of these techniques involve complex process steps and additional infrastructure for selective doping. In addition, earlier works often did not focus on overall performance improvement of MoS_2 FETs without compromising OFF-state characteristics. Moreover, the physical insights into the introduced trap states due to proposed doping technique was missing as well in earlier works.

Although keeping these points in mind, the objective of this paper is to demonstrate, for the first time, an efficient, stable, and yet easy to implement approach of introducing surface charge transfer doping in few-layer MoS_2 using potassium iodide (KI) solution. We will show that the proposed technique significantly lowers the contact resistance, improves the ON-state performance without compromising on FET's stability and the OFF state characteristics. This paper is arranged as follows. Section II discloses experimental and computational approach followed in this paper. Section III will present the experimental findings/observations, validation of proposed doping technique, and develop physical insights using computational results. Section IV will conclude this paper.

Manuscript received April 8, 2019; revised May 6, 2019; accepted May 7, 2019. Date of current version June 19, 2019. This work was supported in part by the Nanoelectronics Network For Research and Application (NNetRA) program of the Ministry of Electronics and Information Technology (MeitY), in part by the Department of Science and Technology (DST), and in part by the Ministry of Human Resource Development (MHRD) Government of India. The review of this paper was arranged by Editor G. L. Snider. *(Corresponding author: Kuruva Hemanjaneyulu.)*

The authors are with the Department of Electronic Systems Engineering, Indian Institute of Science, Bangalore 560012, India (e-mail: hemanjaneyul@iisc.ac.in; mayank@iisc.ac.in).

Color versions of one or more of the figures in this paper are available online at http://ieeexplore.ieee.org.

Digital Object Identifier 10.1109/TED.2019.2916716

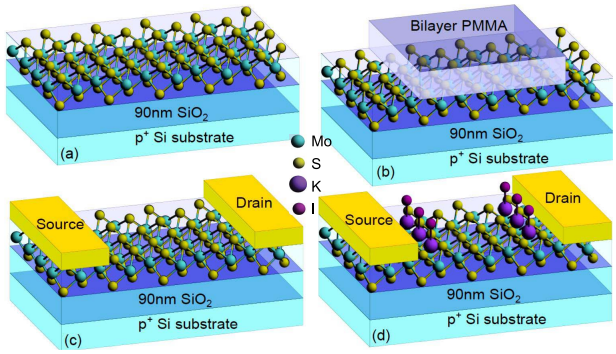

Fig. 1. Process flow for MoS_2 FET with KI doping. (a) Cleaned 90-nm SiO_2/Si substrate with MoS_2 transferred through mechanical exfoliation. (b) Spin coating and patterning bilayer PMMA using e-beam lithography. (c) Ni/Au metal stack deposition using e-beam evaporation followed by liftoff to realize standard backgated FETs. (d) Treatment of KI solution over the device to realize doped backgated FETs.

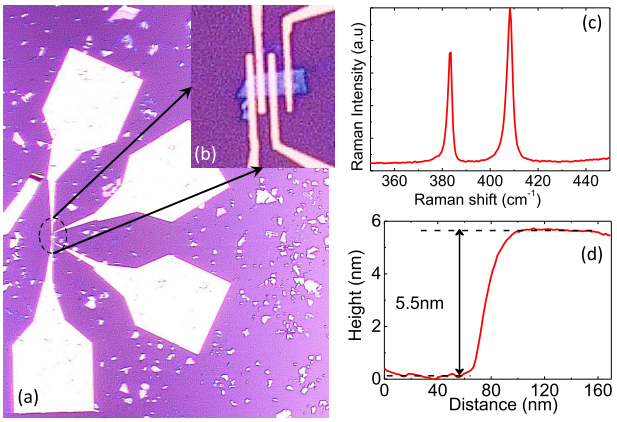

Fig. 2. (a) and (b) Optical image of MoS_2 FET and TLM test structure. Here, the length of the contact region is chosen to be 500 nm, which is well above transfer length for multilayer MoS_2. (c) Raman spectra extracted for MoS_2 crystal post device fabrication. (d) AFM profile for the corresponding flake, which confirms its few-layer nature.

II. Experimental and Computational Procedure

MoS_2 flakes were transferred over a 90 nm SiO_2/P^+ Si substrate using conventional mechanical exfoliation process [19]–[21]. Few-layer flakes were identified using a high-magnification optical microscope and then confirmed by Raman spectroscopy. Atomic force microscopy (AFM) was used to confirm layer thickness and few-layer nature. Back-gated FETs were realized over these selected few-layer flakes to study the impact of KI doping over MoS_2 FETs and TLM test structures with channel lengths down to 300 nm were patterned using e-beam lithography technique with polymethyl methacrylate (PMMA) as the resist material. Using e-beam evaporation, Ni/Au (20/50 nm) was deposited selectively for source/drain contacts followed by metal liftoff and thermal anneal. Furthermore, KI solution with a concentration of 2% is prepared by mixing KI salt in DI water. Various KI concentrations were experimented in the beginning and it was found that 2% results in a maximum improvement in device performance. Increasing KI concentration beyond 2% didn't result in further improvement in the device performance. After complete dissolution of KI salt, the MoS_2 sample was completely immersed into the solution for 5 min at room temperature. A process flow for the KI-doped devices realized in this paper is depicted in Fig. 1. The postdevice fabrication, all the devices were characterized by Raman spectroscopy, AFM, and X-ray photoelectron spectroscopy (XPS) to study material quality, thickness, and impact of doping/electronic state, respectively. Material investigations were followed by electrical characterization. Fig. 2(a) and (b) show optical image of MoS_2 FETs realized in this paper with different channel lengths, Fig. 2(c) shows Raman signal, Fig. 2(d) shows an AFM scan over the flake to confirm few-layer flake thickness. Raman peaks confirm the presence of MoS_2 flake, whereas AFM measured the thickness (5 nm) confirms its few-layer nature. In addition to the experimental analysis, we also studied the effect of doping through band structure analysis, which was carried out by density functional theory (DFT) while using atomistic tool kit (ATK). Band structure was calculated for the following three cases: 1) pristine MoS_2; 2) KI-doped MoS_2; and 3) MoS_2 only with potassium doping. For these calculations, one adsorption atom/molecule is used for every 25 unit cells of MoS_2 crystal. Before band structure calculations, these structures were optimized for least energy states of all the atoms using DFT.

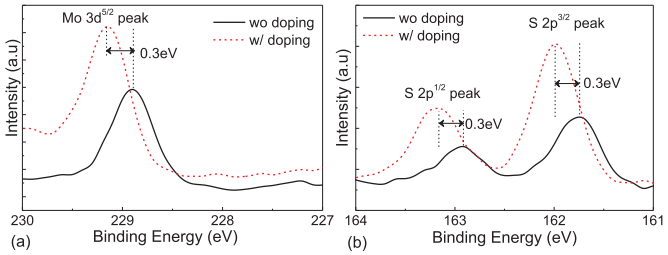

Fig. 3. Comparison of XPS spectra for MoS_2 samples with and without KI doping. Doped sample depicts a blue shift of 0.3 eV in both (a) molybdenum $3d^{5/2}$ peak and (b) sulfur $2p^{1/2}$ and $2p^{3/2}$ peaks, which confirms the ability of KI to dope MoS_2 crystal.

III. Results and Discussion

To confirm the effect of KI doping experimentally, we prepared large area samples with and without KI treatment for ultrahigh resolution XPS analysis. These samples were prepared by mechanical exfoliation over cleaned SiO_2/Si wafer with a very large amount of MoS_2 crystal to have a dense distribution of flakes. Areas densely populated with MoS_2 flakes and having sizes bigger than 2 mm × 2 mm were then selected for XPS analysis. Fig. 3 compares spectrum for both (a) molybdenum 3d peak and (b) sulfur 2p peak. A clear blue shift, from 228.9 to 229.1 eV for molybdenum $3d^{5/2}$ peak and 161.8 to 162.1 eV for sulfur $2p^{3/2}$ peak, after KI doping, is clearly visible. The blue shifts confirm a shift in Fermi energy level toward the conduction band, as reported earlier by Fang *et al.* [12], Yang *et al.* [22], which confirms KI doping of MoS_2 crystal. Relative lower shift of 0.3 eV in comparison with 0.7 eV reported by Fang *et al.* [12], explains the nondegeneracy in KI doping. This will be elaborated later using band structure calculations.

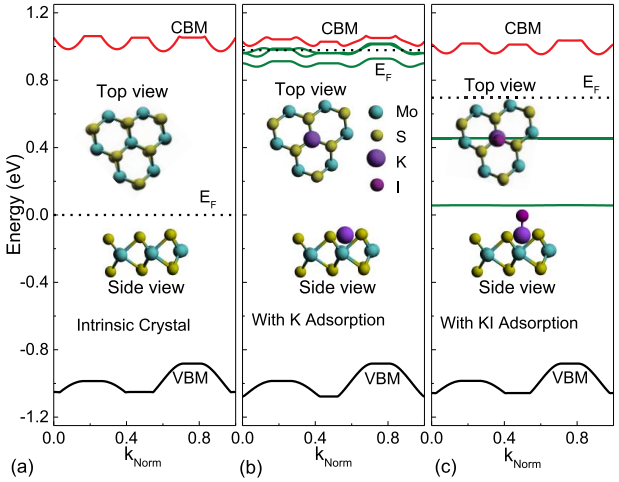

Fig. 4. Comparison of respective band structures. (a) pristine MoS_2 crystal, (b) MoS_2 with K doping, and (c) MoS_2 with KI doping where KI molecule gets adsorbed with K atom over Mo and I atom being present over K atom. Here, green lines represent the induced donor levels due to the adsorption of K atom and KI molecule, in (b) and (c), respectively. Red and black lines represent conduction and valance band minima, respectively; whereas dotted black line represents fermi level.

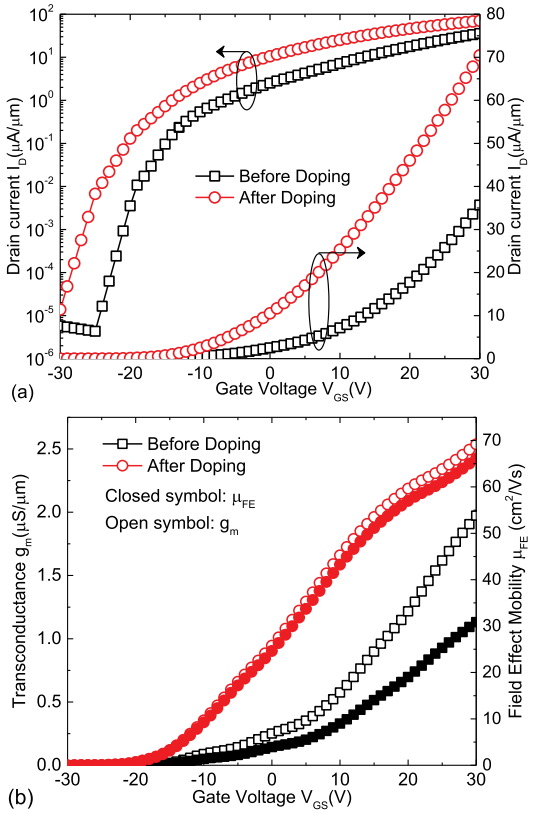

Fig. 5. (a) Drain current versus gate voltage characteristics and (b) transconductance, field-effect mobility versus gate voltage characteristics of MoS_2 FET with $L_G = 300$ nm, extracted at a drain bias $V_{DS} = 0.5$ V, before and after KI doping.

The findings above are further quantified by using band structure calculations, as depicted in Fig. 4, while comparing following three cases (a) pristine MoS_2 crystal, (c) K adsorption over MoS_2 crystal, and (c) KI adsorption over MoS_2 crystal. Fig. 4 (inset) depicts side and top views of the adsorption sites. The adsorption sites for individual cases were disclosed through structure optimization for least energy state using DFT. For 'K' doping, adsorption was found to take place over Mo atom (namely, M site [11]). In this case, MoS_2 was found to become metallic in nature by getting degenerately doped which is evident from the shift in Fermi energy level above the conduction-band minimum. To ensure consistency in our calculation, band structure and adsorption site was reproduced as reported by Ratogi *et al.* [11]. In case of KI molecule, adsorption took place at the M site with K atom bonding with Mo atom and I atom being present over the K atom, as shown in the inset of Fig. 4(c). KI adsorption of MoS_2 crystal has also shown a clear shift in the Fermi energy level closer to the conduction band, as depicted in Fig. 4(c). This confirms n-type doping, which is, however, of nondegenerate nature as evident from a relatively larger separation between Fermi energy level and conduction band minima.

Fig. 5 compares the (a) drain current versus gate voltage and (b) transconductance ($g_m = (dI_D/dV_{GS})$) and field-effect mobility ($\mu_{FE} = (L_G/WC_{OX}) \cdot (g_m/V_{DS})$) versus the gate voltage characteristics of MoS_2 FETs with and without KI doping. Fig. 5(a) shows that devices with KI doping show a marginal negative shift in the threshold voltage, which further confirms n-type doping of the material. The ON current of KI-doped device was found to increase by 2×, which is attributed to lowered contact and channel resistance with KI-based surface charge transfer doping. It should, however, be noted that the OFF-state current of KI-doped devices remain unchanged and was below 10 pA/μm. Fig. 5(b) shows that KI doping results in an improvement of 1.3× in g_m, whereas 2.15× in μ_{FE}. Field-effect mobility has shown to be strongly influenced by the contact resistance [10], [22], reduction of which improves the field-effect mobility. We also attribute the improvement in field-effect mobility and improvement in ON current to the reduced contact resistance due to the KI doping at the contact-channel edge. The improved mobility also signifies that the proposed doping does not lead to doping dependent mobility degradation as opposed to the conventional ion implantation based doping.

To validate our arguments above, further analysis has been carried out by extracting contact resistance and approximate dopant density. The contact resistance has been extracted using Y-Function method as earlier reported by Ghibaudo [23] and Fleury *et al.* [24] for nanoscale MOSFETs, which was later validated for MoS_2 FETs by Chang *et al.* [25]. The comparison of Y-function resistance with gate voltage for devices with and without KI doping is presented in Fig. 6. Without KI doping, the least contact resistance was found to be 2.6 k$\Omega\mu$m. The same reduced to 0.75 k$\Omega\mu$m, which is 3.5× reduction, in case of KI-doped MoS_2 FETs. Given that the OFF-state current has remain unchanged, it can be concluded that KI doping took place majorly around the contact edges, which lowers the contact resistances by enhancing carrier tunneling from contact edges, thereby improves the overall performance of MoS_2 FETs. Approximate dopant density ($n_{Eff} = |C_{OX} \cdot (V_{TH\text{-}After} - V_{TH\text{-}Before})|$), which assumes no influence of contact over threshold voltage of the device, was found to be 1×10^{12} cm^{-2},

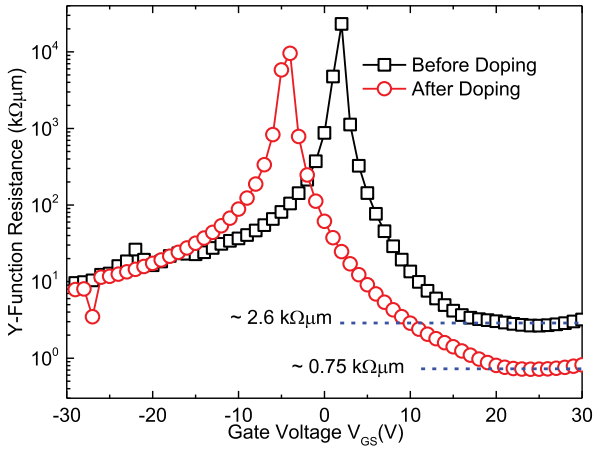

Fig. 6. Comparison of Y-Function extracted contact resistance before and after KI doping. Contact resistance of MoS_2 FETs ($L_G = 300$ nm) was extracted at a drain bias $V_{DS} = 0.5$ V.

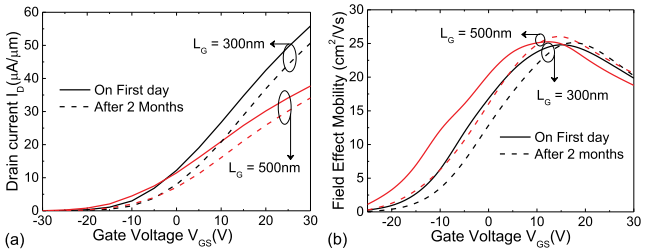

Fig. 7. (a) Input characteristics and (b) field-effect mobility of MoS_2 FET measured immediately after the KI treatment and 2 months post-KI treatment for a device with $L_G = 300$ nm at a drain bias $V_{DS} = 0.5$ V.

which further confirms the nondegeneracy in the doping. This very nature of nondegenerate doping and doping around the contact edge are responsible for maintaining ON to OFF current ratios well above 10^5 across all the KI-doped MoS_2 FETs.

From a practical standpoint, introduced doping is required to be stable against environment conditions. In earlier works, the ambient environment has shown to influence the dopant stability, of charge transfer doping, over time [12]–[14]. To investigate the dopant stability, electrical measurements over doped devices were performed after 2 months of the KI treatment. Fig. 7 compares the input characteristics and field-effect mobility. Input characteristics show a marginal shift in threshold voltage and a slight reduction in ON current. Marginal change in threshold voltage confirms doping stability, while a slight reduction in ON current can be attributed to repeated stressing of the device. Given that the peak channel mobility remains unchanged after 2 months, it can be concluded that degradation in channel properties was largely missing. These results confirm the stability of the proposed doping scheme against environmental conditions.

Fig. 8 shows the input characteristics of KI-doped device measured under saturation condition to extract maximum ON-current at $L_G = 300$ nm and least ON to OFF current ratio. The device shows a current density of 500 μA/μm, maximum transconductance of 13.4 μS/μm while maintaining

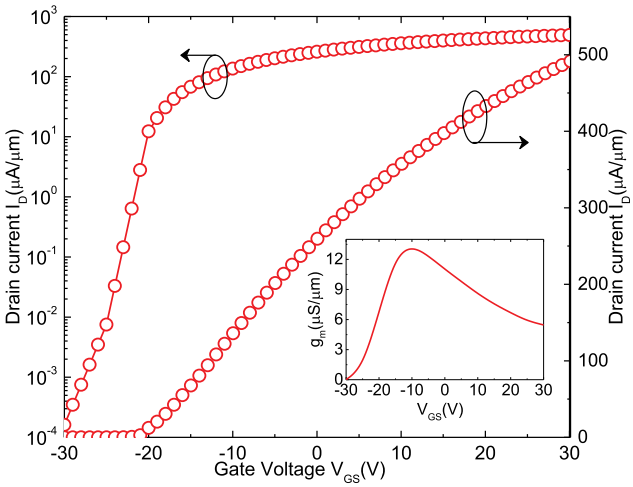

Fig. 8. KI doped MoS_2 FET's drain current versus gate voltage characteristics extracted at $V_{DS} = 3$ V, showing the current density of 500 μA/μm. Inset shows the corresponding transconductance variation, with maximum of 13.38 μS/μm.

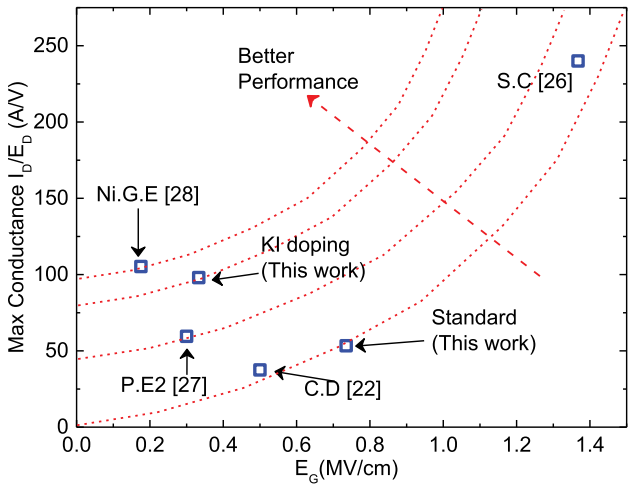

Fig. 9. Comparison of maximum conductance with gate field (in linear region) of devices realized in this paper with best techniques reported in the literature. S.C.: Scandium contacted FET [26]. P.E2: Phase engineered 7.5-nm stripes across 90 nm channel FET [27]. Ni.G.E.: Ni treated graphene electrodes [28]. C.D.: Chlorine doping [22].

ON to OFF current ratio greater than 10^6. Fig. 9 compares the maximum conductance achieved in this paper with the existing literature. Maximum conductance in the linear regime of FET operation versus gate field is chosen for comparison to enable normalization in terms of both drain and gate fields. Dashed lines depict approximate square law rise in the conductance with gate field and represent an equal-performance contour. From these characteristics, it can be noted that KI doping outperforms most of the techniques reported earlier. Finally, Table I summarizes transistor's figure-of-merit parameters of KI-doped MoS_2 FET in this paper and compares with the figure-of-merit parameters reported in other contact engineering reports. It can be clearly noted that KI doping offers overall performance improvement while other techniques fail to address one or the other key transistor performance parameter. In most of the cases, for example,

TABLE I
COMPARISON OF PERFORMANCE METRICS ACHIEVED IN THIS PAPER WITH THE EARLIER REPORTS. P.E1: PHASE ENGINEERING IN CONTACT REGION [10]. G.E.: GRAPHENE ELECTRODES [29]. S.T.: SULFUR TREATMENT [30]

Reference	I_{ON} $(\mu A/\mu m)$	R_C $(k\Omega\mu m)$	μ_{FE} (cm^2/Vs)	Max g_m $(\mu S/\mu m)$	$\frac{I_{ON}}{I_{OFF}}$
P.E1 [10]	85	0.2	46	3.8	10^7
P.E2 [27]	1200	-	25	-	10^2
G.E [29]	830	0.54	104	-	10^3
C.D [22]	460	0.5	60	-	10^5
Ni.G.E [28]	420	0.2	80	-	10^5
S.T [30]	170	4.65	28.4	-	10^6
KI Doping	500	0.75	73	13.38	10^6

OFF state current was compromised by orders of magnitude in interest of improving ON state performance. However, with KI doping, the OFF state behavior remains unchanged.

IV. CONCLUSION

We report a stable charge transfer doping technique for MoS_2 thin flakes using KI solution. KI doping, which results in adsorption of KI molecule over MoS_2 surface at the M site, was found to nondegenerately dope MoS_2 layer near the S/D metal and channel edge. This allowed KI doping to significantly lower the contact resistance ($3.5\times$) and improve ON current as well as channel mobility ($2\times$). Using KI doping contact resistance as low as 0.75 $k\Omega\mu$m, ON current up to 500 μA/μm and field effect mobilities above 70 cm^2/Vs was achieved, while maintaining ON to OFF ratio well above 10^6. Stability of KI doping against the environmental conditions was also validated by measuring the doped devices after 2 months.

REFERENCES

[1] K. S. Novoselov *et al.*, "Electric field effect in atomically thin carbon films," *Science*, vol. 306, no. 5696, pp. 666–669, 2004. [Online]. Available: http://science.sciencemag.org/content/306/5696/666

[2] Y. Zhang, Y.-W. Tan, H. L. Stormer, and P. Kim, "Experimental observation of the quantum hall effect and berry's phase in graphene," *Nature*, vol. 438, pp. 201–204, Nov. 2005. doi: 10.1038/nature04235.

[3] K. S. Novoselov *et al.*, "Two-dimensional gas of massless dirac fermions in graphene," *Nature*, vol. 438, pp. 197–200, Nov. 2005. doi: 10.1038/nature04233.

[4] Q. H. Wang, K. Kalantar-Zadeh, A. Kis, J. N. Coleman, and M. S. Strano, "Electronics and optoelectronics of two-dimensional transition metal dichalcogenides," *Nature Nanotechnol.*, vol. 7, pp. 699–712, Nov. 2012. doi: 10.1038/nnano.2012.193.

[5] K. F. Mak, C. Lee, J. Hone, J. Shan, and T. F. Heinz, "Atomically thin MoS_2: A new direct-gap semiconductor," *Phys. Rev. Lett.*, vol. 105, no. 13, Sep. 2010, Art. no. 136805. doi: 10.1103/PhysRevLett.105.136805.

[6] A. Castellanos-Gomez, M. Poot, G. A. Steele, H. S. J. van der Zant, N. Agraït, and G. Rubio-Bollinger, "Elastic properties of freely suspended MoS_2 nanosheets," *Adv. Mater.*, vol. 24, no. 6, pp. 772–775, Feb. 2012. doi: 10.1002/adma.201103965.

[7] S. Bertolazzi, J. Brivio, and A. Kis, "Stretching and breaking of ultrathin MoS_2," *ACS Nano*, vol. 5, no. 12, pp. 9703–9709, Nov. 2011. doi: 10.1021/nn203879f.

[8] J. Pu, Y. Yomogida, K.-K. Liu, L.-J. Li, Y. Iwasa, and T. Takenobu, "Highly flexible MoS_2 thin-film transistors with ion gel dielectrics," *Nano Lett.*, vol. 12, no. 8, pp. 4013–4017, Jul. 2012. doi: 10.1021/nl301335q.

[9] B. Liu, L. Chen, G. Liu, A. N. Abbas, M. Fathi, and C. Zhou, "High-performance chemical sensing using schottky-contacted chemical vapor deposition grown monolayer MoS_2 transistors," *ACS Nano*, vol. 8, no. 5, pp. 5304–5314, Apr. 2014. doi: 10.1021/nn5015215.

[10] R. Kappera *et al.*, "Phase-engineered low-resistance contacts for ultrathin MoS_2 transistors," *Nature Mater.*, vol. 13, pp. 1128–1134, Aug. 2014. doi: 10.1038/nmat4080.

[11] P. Rastogi, S. Kumar, S. Bhowmick, A. Agarwal, and Y. S. Chauhan, "Doping strategies for monolayer MoS_2 via surface adsorption: A systematic study," *J. Phys. Chem. C*, vol. 118, no. 51, pp. 30309–30314, Nov. 2014. doi: 10.1021/jp510662n.

[12] H. Fang *et al.*, "Degenerate n-doping of few-layer transition metal dichalcogenides by potassium," *Nano Lett.*, vol. 13, no. 5, pp. 1991–1995, May 2013. doi: 10.1021/nl400044m.

[13] H.-M. Li *et al.*, "Ultimate thin vertical p–n junction composed of two-dimensional layered molybdenum disulfide," *Nature Commun.*, vol. 6, Mar. 2015, Art. no. 6564. doi: 10.1038/ncomms7564

[14] D. Kiriya, M. Tosun, P. Zhao, J. S. Kang, and A. Javey, "Air-stable surface charge transfer doping of MoS_2 by benzyl viologen," *J. Amer. Chem. Soc.*, vol. 136, no. 22, pp. 7853–7856, May 2014. doi: 10.1021/ja5033327.

[15] D. Sarkar *et al.*, "Functionalization of transition metal dichalcogenides with metallic nanoparticles: Implications for doping and gas-sensing," *Nano Lett.*, vol. 15, no. 5, pp. 2852–2862, Feb. 2015. doi: 10.1021/nl504454u.

[16] J. D. Lin *et al.*, "Electron-doping-enhanced trion formation in monolayer molybdenum disulfide functionalized with cesium carbonate," *ACS Nano*, vol. 8, no. 5, pp. 5323–5329, May 2014. doi: 10.1021/nn501580c.

[17] S. Fathipour *et al.*, "Record high current density and low contact resistance in MoS_2 FETs by ion doping," in *Proc. Int. Symp. VLSI Technol., Syst. Appl. (VLSI-TSA)*, Apr. 2016, pp. 1–2.

[18] M. S. Choi *et al.*, "Lateral MoS_2 p–n junction formed by chemical doping for use in high-performance optoelectronics," *ACS Nano*, vol. 8, no. 9, pp. 9332–9340, Aug. 2014. doi: 10.1021/nn503284n.

[19] K. S. Novoselov *et al.*, "Two-dimensional atomic crystals," *Proc. Nat. Acad. Sci. USA*, vol. 102, no. 30, pp. 10451–10453, 2005. [Online]. Available: http://www.pnas.org/content/102/30/10451

[20] R. F. Frindt, "Single crystals of MoS_2 several molecular layers thick," *J. Appl. Phys.*, vol. 37, no. 4, pp. 1928–1929, 1966. doi: 10.1063/1.1708627.

[21] R. Fivaz and E. Mooser, "Mobility of charge carriers in semiconducting layer structures," *Phys. Rev.*, vol. 163, no. 3, pp. 743–755, Nov. 1967. doi: 10.1103/PhysRev.163.743.

[22] L. Yang *et al.*, "High-performance mos2 field-effect transistors enabled by chloride doping: Record low contact resistance (0.5 k$\omega\mu$m) and record high drain current (460 $\mu a/\mu m$)," in *Symp. VLSI Technol. (VLSI-Technol.), Dig. Tech. Papers*, Jun. 2014, pp. 1–2.

[23] G. Ghibaudo, "New method for the extraction of MOSFET parameters," *Electron. Lett.*, vol. 24, no. 9, pp. 543–545, Apr. 1988.

[24] D. Fleury, A. Cros, H. Brut, and G. Ghibaudo, "New Y-function-based methodology for accurate extraction of electrical parameters on nano-scaled MOSFETs," in *Proc. IEEE Int. Conf. Microelectron. Test Struct.*, Mar. 2008, pp. 160–165.

[25] H.-Y. Chang, W. Zhu, and D. Akinwande, "On the mobility and contact resistance evaluation for transistors based on MoS_2 or two-dimensional semiconducting atomic crystals," *Appl. Phys. Lett.*, vol. 104, no. 11, 2014, Art. no. 113504. doi: 10.1063/1.4868536.

[26] S. Das, H.-Y. Chen, A. V. Penumatcha, and J. Appenzeller, "High performance multilayer MoS_2 transistors with scandium contacts," *Nano Lett.*, vol. 13, no. 1, pp. 100–105, Dec. 2013. doi: 10.1021/nl303583v.

[27] A. Nourbakhsh *et al.*, "Mos2 field-effect transistor with sub-10 nm channel length," *Nano Lett.*, vol. 16, no. 12, pp. 7798–7806, Dec. 2016. doi: 10.1021/acs.nanolett.6b03999.

[28] W. S. Leong, X. Luo, Y. Li, K. H. Khoo, S. Y. Quek, and J. T. L. Thong, "Low resistance metal contacts to MoS_2 devices with nickel-etched-graphene electrodes," *ACS Nano*, vol. 9, no. 1, pp. 869–877, Dec. 2015. doi: 10.1021/nn506567r.

[29] Y. Liu *et al.*, "Pushing the performance limit of sub-100 nm molybdenum disulfide transistors," *Nano Lett.*, vol. 16, no. 10, pp. 6337–6342, Aug. 2016. doi: 10.1021/acs.nanolett.6b02713.

[30] S. Bhattacharjee, K. L. Ganapathi, D. N. Nath, and N. Bhat, "Surface state engineering of metal/MoS_2contacts using sulfur treatment for reduced contact resistance and variability," *IEEE Trans. Electron Devices*, vol. 63, no. 6, pp. 2556–2562, Jun. 2016.